IEEE Access
Multidisciplinary | Rapid Review | Open Access Journal

Received 28 February 2024, accepted 6 March 2024, date of publication 11 March 2024, date of current version 15 March 2024.

Digital Object Identifier 10.1109/ACCESS.2024.3375346

RESEARCH ARTICLE

Efficient Adaptive Regulation Strategy for Control Position of Induction Motors

RUBEN TAPIA-OLVERA[1], ANTONIO VALDERRABANO-GONZALEZ[2], (Member, IEEE), AND FRANCISCO BELTRAN-CARBAJAL[3]

[1]Department of Electrical Energy, Universidad Nacional Autónoma de México, Mexico City 04510, Mexico
[2]Facultad de Ingeniería, Universidad Panamericana, Zapopan, Jalisco 45010, Mexico
[3]Department of Energy, Universidad Autónoma Metropolitana, Unidad Azcapotzalco, Mexico City 02200, Mexico

Corresponding author: Antonio Valderrabano-Gonzalez (avalder@up.edu.mx)

This work was supported by Universidad Panamericana through the Fondo Fomento a la Investigación UP 2023 under Project UP-CI-2023-GDL-09-ING.

ABSTRACT In this paper, we introduce an efficient adaptive algorithm based on B-spline neural networks for trajectory tracking of angular position for industrial induction motors. This strategy is developed in a two-axis reference frame and the regulation algorithm is based on four main stages: a) flux observer; b) internal control loop; c) determination of required electrical currents and; d) calculation of the three-phase input voltages. The strategy considers an algebraic regulation scheme based on the model. The control parameters are tuning online to attain the best dynamic behavior, besides, the proposed adaptive controller is subject to non-modeled components as an 84-pulse voltage source converter included in this study. These two aspects make the main contribution of this article. The proposed high-performance strategy for trajectory tracking of angular position is demonstrated by simulation results using the parameters of two induction motors of 500 hp and 50 hp, respectively.

INDEX TERMS Adaptive regulation, angular position trajectory tracking, efficient driver, high performance, induction motors.

I. INTRODUCTION

Nowadays, the industry demands more efficient strategies for motor operation, particularly in highly demanding applications. In this context, the induction machine continues to gain more significance in industrial processes where it was not widely utilized until a few years ago, thanks to the rapid development of power electronics. Consequently, any study must consider the impact of using power electronic devices. The control of angular rotor position is a crucial requirement in the industry, typically addressed by direct current (DC) motors or permanent magnet synchronous motors [1]. However, induction motors could also participate in these rigorous tasks; nevertheless, their operation must be guaranteed in terms of reliability, security, and efficiency. Moreover, new growing applications such as electric vehicles see the induction motors as a very important alternative, but the advantages of their use must be guaranteed by the control strategy [2].

Important control strategies for induction motors are available in scientific literature such as field orientation control, direct torque control, model predictive control, sliding mode control, and intelligent control techniques. However, the dependency on model parameters, complexity, and highly demanding computational effort of intelligent techniques causes a gap that needs to be covered with new efficient strategies including the effect of power electronic drives [3]. A strategy for rotor position control of induction motors based on field-oriented control, incorporating a scheme that utilizes neural networks to address time-varying dynamics and a non-linear structure is presented in [4]. Additionally, it involves fractional-order proportional-integral controllers, which have been tuned using an artificial bee colony optimization algorithm. In [5] an adaptive scheme based on fuzzy neural networks is presented for rotor position control of induction motors which emulates the conventional proportional-integral (PI) controller. That scheme requires

The associate editor coordinating the review of this manuscript and approving it for publication was Pinjia Zhang.

two groups of parameters to be trained in hidden layers to reach the desired control performance, which was adapted for the study case. In the same line of adaptive control techniques, [6] presents a control of induction motors using an adaptive high gain observer based on a model reference adaptive system. The success of that scheme lies in the correct estimation of the model and a speed adaptation mechanism. In [7], speed control of induction motor (IM) by fractional sliding mode control in combination with radial basis function (RBF) neural network. In that case, the RBF configuration is formed with three layers, five nodes in the hidden layer, and two input signals, the error and its derivative. The RBF's output feeds the fractional sliding mode control to obtain the optimal control rate and to reduce the speed-observed chatter of the bearing-less IM. A common feature of these schemes is the constraints that must be included for each neural network architecture and learning rule. Which does not necessarily have the desired best performance when the test system changes. Besides that, relevant neural network architectures are proposed to improve the control algorithm performance, mainly to avoid the problems related to delays in the transmission of information, uncertainties of parameters, and some possible faults in the neuron connection of the neural network architecture as present in [8] and, [9]. An analysis of a possible reconfiguration of the neural network architecture due to the disconnection of some neurons inside the hidden layers could be evaluated as present in [8].

On the other hand, the impact of the power electronic drivers in the control scheme, also, has been evaluated. In [10] a nine-switch inverter is used to regulate two IM using model predictive control but to overcome problems of closed-loop instability in the design stage the cost function was formulated as a Lyapunov energy function. In addition, in [11] a driver based on a dual inverter configuration is proposed which compensates for the reactive power of the five-phase induction motor. In that scheme, an inverter with a capacitor is controlled to compensate for the increasing reactive voltage drop inside the motor as the speed increases. Paper [12] presents a proposal of a voltage source inverter to control the speed and power flow of a squirrel-cage induction motor. The features that they try to solve are to create a smooth startup, a stable control strategy, and a power factor correction using capacitor banks. In other special configurations of drivers for variable pole–phase induction motors, the problems related to magnified space harmonics at air gap and the harmonic offset injected in reference waves for pulse width modulation try to reduce in [13] employing a three-switch leg (3SL)/phase inverter topology.

Thus, efficient control strategies for induction motors are an open research topic, where demand new proposed schemes operating harmoniously with driver based on power electronics covering a wide range of operation conditions of IM, motor's parameters uncertainties, non-linear phenomena present, reduction of parameter dependency on the control design stage, diminished sinusoidal waveform distortion and reactive power consumption. And the possibility of rotor position control without external mechanical elements coupling with the shaft of the induction motor. The main contributions of this paper are i) a new control strategy for the rotor position of induction motors free of gears based on algebraic formulation; ii) adaptive tuning of control gains to adjust itself to uncertainties and non-modeled phenomena based on B-spline neural networks (BSNN); iii) efficient operation of 84-pulse voltage source converter (VSC) drive to feed the induction motor and cover any requirement of the position and load torque.

The motor driver is crucial for precise position and speed regulation in electric motors. Serving as the interface between control algorithms and the motor itself, it modulates the electrical signals, ensuring accurate motor performance. This precision is essential in applications ranging from industrial automation to robotics, where consistent and controlled motion is paramount for optimal efficiency and functionality.

In the context of using three-phase motors, several merit figures are commonly used to assess the performance and efficiency of the motor. These merit figures include the Power Factor (PF), which is the cosine of the angle between the voltage and current waveforms in a three-phase system and represents the ratio of real power (useful power) to apparent power (total power); Displacement Power Factor (DPF), that considers the phase shift between the voltage and current waveforms; Total Harmonic Distortion (THD), which quantifies the harmonic distortion in the voltage or current waveform. Power per Phase (P/phase), as the average power consumed by each phase in a three-phase system. The Regular monitoring and analysis of these parameters are essential for maintaining a reliable and efficient three-phase motor system.

VSCs have been implemented in industry for a lot of applications, including STATCOM, active filters, UPS, and machine drives among others [14]. Nevertheless, most of them use a topology that can present a high THD due to low number of pulses or levels. Multipulse VSCs used for high power configurations have demonstrated their capability to improve conversion efficiency, such as in [15], however, the main application is the reactive compensation for voltage regulation, but fast variations related to high-power motor position control have not been verified. The utilization of an 84-pulse Voltage Source Converter (VSC) extends its applicability across various scenarios where an inverter is essential. While conventional inverters with lower pulse counts are commonly employed, the distinctive feature of an 84-pulse VSC lies in its ability to offer finer control and smoother waveform output. This makes it particularly advantageous in applications demanding higher precision, reduced harmonic distortion, and enhanced overall performance compared to inverters with lower pulse count. However, this expected performance could take advantage of the high-performance adaptive control algorithm accomplishing it. For this reason,

the proposed position control is designed based on an induction motor model, but the integration of B-spline neural networks reaches robustness and adaptability. The adaptability and fast learning capability of the BSNN allow improvement in the performance of the proposed control scheme in contrast to other important algorithms presented in the literature. In this way, this proposed control strategy is derived to improve two fundamental aspects as a response to motors industry applications: i) secure and reliable expansion of the induction motor industrial applications in tasks of trajectory tracking position control and ii) propose efficient controllers which have fast response, robustness and adaptive behavior with reduced dependence on models, motor parameters and prior knowledge of severe transient events.

As can be analyzed in the previous paragraphs, the global industry is constantly evolving, enhancing various aspects of its operational efficiency, cost-effectiveness, and environmental footprint. In this context, induction motors are gaining prominence due to their superior features in design, operation, and maintenance, especially in applications that were less common in previous decades. However, accompanying this growth, the motor is exposed to more complex and highly demanding scenarios in terms of load variability, and severe disturbances not considered in the design stage. Thus, the control strategy requires attributes such as faster and more efficient responses. In this way, the proposed strategy is focused to cover two fundamental aspects in considering those requirements: i) secure and reliable expansion of the induction motor industrial applications in tasks of trajectory tracking position control and ii) propose efficient controllers which have fast response, robustness and adaptive behavior with reduced dependence on models, motor parameters and prior knowledge of severe transient events. In this paper, these features are attained with the correct definition of the adaptive control scheme based on B-spline neural networks working synergically with a VSC of 84 pulses. The election of this neural network topology covers these aspects due to architecture based on a hidden layer and fast response exhibiting an adaptive behavior using an instantaneous learning rule working online with the motor. Hence, it is possible to learn of new events, operation conditions or possible perturbations. Unlike other neural network architecture, the offline training of this configuration does not require an extensive set of input-output data. This stage is executed to define the operation in a steady state, the learning rate, and the convergence of the instantaneous learning rule. The rapid response is achieved by employing a smaller number of neurons, specifically, three in the proposed scheme's hidden layer. This choice strikes a balance between achieving high dynamic performance and minimizing the computational load. Moreover, the performance of the control adaptive strategy does not depend on the case of the induction motor in terms of power, voltage, or electrical current.

This research paper introduces an Electric Motor Drive System designed to accurately follow the required voltage and current specified by the load. Merit figures such as frequency profile and voltage profile depict the necessary variations, while the power factor serves as an indicator of the excellent performance achieved by the Voltage Source Converter (VSC). To attain this performance, the proposed controller along with the B-Spline Neural Networks are introduced with an effective architecture and online learning rule. Thus, the proposed control algorithm guarantees high performance in steady and transient states, facing uncertainties and nonmodeled nonlinear dynamics as the ones related to 84-pulse VSC components which were not included in the control design stage. Moreover, the B-spline neural network architecture and its learning rule can deal with fast perturbations due to the low number of calculations required to determine the best position control parameters.

This paper is organized as follows: Section I outlines the problem addressed by this research. Section II introduces the induction motor model used. Section III provides detailed information on the position control scheme. Section IV illustrates the 84-pulse driver, employed for precise motor control. Section V presents the regulatory results obtained, and finally, Section VI remarks the research findings of this paper.

II. MODELING OF THE INDUCTION MOTOR FOR REGULATING PURPOSES

Considering the model in a three-phase reference frame of the induction motor it is possible using the transformation presented in section IV-A arrive to at a model in two axes. Thus, the induction machine for regulation purposes could be modeled in this reference frame of two axes as,

$$\begin{aligned}
\frac{dI_{Sa}}{dt} &= -\gamma I_{Sa} + \eta\beta\psi_{Ra} + \beta n_p\omega\psi_{Rb} + \frac{1}{\sigma L_S}u_{sa} \\
\frac{dI_{Sb}}{dt} &= -\gamma I_{Sb} + \eta\beta\psi_{Rb} - \beta n_p\omega\psi_{Ra} + \frac{1}{\sigma L_S}u_{sb} \\
L_R\frac{d\psi_{Ra}}{dt} &= -R_R\psi_{Ra} - L_R n_p\omega\psi_{Rb} + R_R M I_{Sa} \\
L_R\frac{d\psi_{Rb}}{dt} &= -R_R\psi_{Rb} + L_R n_p\omega\psi_{Ra} + R_R M I_{Sb} \\
\frac{d\theta}{dt} &= \omega \\
J\frac{d\omega}{dt} &= \frac{n_p M}{L_R}(I_{Sb}\psi_{Ra} - I_{Sa}\psi_{Rb}) - b\omega - \tau_L
\end{aligned} \tag{1}$$

where θ is the angular position; ω is the rotor speed; i_{sa} and i_{sb} are the stator currents per phase; ψ_{Ra} and ψ_{Rb} are the magnetic flux in the rotor; u_{sa} and u_{sb} are the stator voltages per phase, which act as input control variables; τ_L is the load torque. Also, L_R and R_R are the rotor inductance and resistance per phase, respectively; L_S and R_S are the stator inductance and resistance per phase, respectively; M is the mutual inductance constant; J is the rotor inertia moment; b viscous damping coefficient; n_p is the number of pairs poles. Some auxiliary parameters were defined based

on machine data as,

$$\eta = \frac{R_R}{L_R}, \quad \gamma = \frac{M^2 R_R}{\sigma L_R^2 L_S} + \frac{R_S}{\sigma L_S}$$
$$\beta = \frac{M}{\sigma L_R L_S}, \quad \sigma = 1 - \frac{M^2}{L_R L_S}$$

Now, a complex coordinate representation of the induction motor dynamics can be derived as

$$\begin{aligned} \frac{dI_S}{dt} &= \beta(\eta - jn_p\omega)\psi_R - \gamma I_S + \frac{1}{\rho L_S}u_s \\ \frac{d}{dt}|\psi_R|^2 &= -2\eta|\psi_R|^2 + 2\eta M \mathrm{Re}(\bar{\psi} I_S) \\ \frac{d\theta}{dt} &= \omega \\ J\frac{d\omega}{dt} &= \frac{n_p M}{L_R}\mathrm{Im}(\bar{\psi} I_S) - b\omega - \tau_L \end{aligned} \tag{2}$$

The variables in the complex notation for this representation of the induction motor are,

$$u_s = u_{sa} + ju_{sb} = |u_s|e^{j\phi_1} \tag{3}$$
$$I_S = I_{Sa} + jI_{Sb} = |I_S|e^{j\phi_2} \tag{4}$$
$$\psi_R = \psi_{Ra} + j\psi_{Rb} = |\psi_R|e^{j\phi_3} \tag{5}$$
$$|\psi_R|^2 = {\psi_{Ra}}^2 + {\psi_{Rb}}^2 \tag{6}$$
$$|I_S|^2 = {I_{Sa}}^2 + {I_{Sb}}^2 \tag{7}$$
$$\lambda = \arctan\left(\frac{\psi_{Rb}}{\psi_{Ra}}\right) \tag{8}$$
$$\rho = \arctan\left(\frac{I_{Sb}}{I_{Sa}}\right) \tag{9}$$
$$\mathrm{Re}\left(\bar{\psi}_R I_S\right) = \psi_{Ra} I_{Sa} + \psi_{Rb} I_{Sb} \tag{10}$$
$$\mathrm{Im}\left(\bar{\psi}_R I_S\right) = \psi_{Ra} I_{Sb} - \psi_{Rb} I_{Sa} \tag{11}$$

where $\bar{\psi}_R$ is the conjugate complex of ψ_R. Re $(\cdot)$ and Im $(\cdot)$ are the real and imaginary of the complex number $(\cdot)$, respectively.

III. ADAPTIVE SCHEME FOR POSITION CONTROL OF INDUCTION MOTORS

In this paper, the proposed control scheme for adaptive angular position tracking consists of the design of a controller defined by two stages. First, the angular position of the motor shaft is conducted to a desired position, $\theta^*(t)$, trajectory by the regulation of the stator currents. The second stage consists of a control loop to define the stator currents monitoring the required paths of the stator currents in the first stage $I_{Sa}^*(t)$ and $I_{Sb}^*(t)$, through the voltages of the stator.

A. INTERNAL CONTROL LOOP

First consider the complex model, (2), of the induction motor to design an angular position and magnetic flux control scheme, using the stator phase currents I_{Sa} and I_{Sa} as control variables. For control design purposes, can be rewritten as,

$$\frac{d^2\theta}{dt^2} = \frac{n_p M}{JL_R}u_\theta - \frac{b}{J}\omega - \frac{1}{J}\tau_L \tag{12}$$
$$\frac{d}{dt}\Psi = -\frac{2R_R}{L_R}\Psi + \frac{2R_R M}{L_R}u_\Psi \tag{13}$$

with $\Psi = |\psi|^2$.

To follow reference trajectories for the angular position $\theta^*(t)$ and the square flow modulus $\Psi^*(t)$ we propose auxiliary controllers as,

$$\begin{aligned} u_\theta = \frac{JL_R}{n_p M}\Bigg[&\frac{d^2\theta^*}{dt^2} - \alpha_{3,\theta}\frac{d}{dt}e_\theta - \alpha_{2,\theta}e_\theta - \alpha_{1,\theta}\int_0^t e_\theta dt \\ &- \alpha_{0,\theta}\int_0^t\int_0^t e_\theta(\tau)d\tau dt + \frac{b}{J}\omega\Bigg] \end{aligned} \tag{14}$$

$$\begin{aligned} u_\Psi = \frac{L_R}{2R_R M}\Bigg[&\frac{d\Psi^*}{dt} - \alpha_{2,\Psi}e_\Psi - \alpha_{1,\Psi}\int_0^t e_\Psi dt \\ &- \alpha_{0,\Psi}\int_0^t\int_0^t e_\Psi(\tau)d\tau dt + \frac{2R_R}{L_R}\Psi\Bigg] \end{aligned} \tag{15}$$

where

$$\begin{aligned} e_\theta &= \theta - \theta^* \\ e_\Psi &= \Psi - \Psi^* \end{aligned} \tag{16}$$

The parameter values of control are selected by the next proposed stable polynomials for the close loop dynamics,

$$P_\theta(s) = (s + p_\theta)^4 = s^4 + 4p_\theta s^3 + 6p_\theta^2 s^2 + 4p_\theta^3 s + p_\theta^4 \tag{17}$$

$$P_\Psi(s) = (s + p_\Psi)^3 = s^3 + 3p_\Psi s^2 + 3p_\Psi^3 s + p_\Psi^3 \tag{18}$$

thus,

$$\begin{aligned} \alpha_{0,\theta} &= p_\theta^4, \quad \alpha_{1,\theta} = 4p_\theta^3 \\ \alpha_{2,\theta} &= 6p_\theta^2, \quad \alpha_{3,\theta} = 4p_\theta \\ \alpha_{0,\Psi} &= p_\Psi^3, \quad \alpha_{1,\Psi} = 3p_\Psi^2 \end{aligned} \tag{19}$$

$$\alpha_{2,\Psi} = 3p_\Psi \tag{20}$$

with p_θ, $p_\Psi > 0$. To attain an adaptive performance of the proposed control scheme, in this paper, a strategy based on B-spline neural networks is introduced to overcome the inherent problem in the control design stage of parameters uncertainty and unmodeled nonlinear phenomena.

First, the parameters $p_/theta$ and $p_/Psi$ are defined with a constant value greater than zero which could even remain constant. However, the dynamic performance of the control algorithm might be degraded when facing other complex operation conditions as described previously or the presence of uncertainties or nonmodeled phenomena. Thus, we defined in the proposed scheme an initial value of these two control gains, and the training procedure for the proposed B-spline neural network architecture begins in an offline way to ensure steady-state performance, hence the training algorithm itself searches for the best gain values to cover some operation conditions and unknown transient events. Once this is done, in the online stage, the instantaneous learning rule (explained

in section III-E), accompanies the BSNN behavior which causes the control gains to be now dynamic, therefore, the optimum values are determined depending on the scenarios to which the induction motor is subjected. Under this condition, the proposed algorithm alone determines the optimal values of the control gains, avoiding the dependence on the model and parameters.

Now, under this consideration, the reference signals of electrical currents are defined as,

$$I_S^* = \frac{\psi_R}{\Psi}(u_\Psi + j u_\theta) \tag{21}$$

thus,

$$\begin{aligned} I_{Sa}^* &= \frac{1}{\Psi}(\psi_{Ra} u_\Psi - \psi_{Rb} u_\theta) \\ I_{Sb}^* &= \frac{1}{\Psi}(\psi_{Rb} u_\Psi + \psi_{Ra} u_\theta) \end{aligned} \tag{22}$$

B. REQUIRED INPUT VOLTAGE FOR POSITION CONTROL

Considering the dynamics of electrical currents, I_{Sa} and I_{Sb}, described in (1) and based on the required trajectories of these variables, (22), it is proposed to determine the input voltages with adaptive control parameters, $\alpha_{i,a}$, and $\alpha_{i,b}$,

$$\begin{aligned} u_{sa} = \sigma L_S \Bigg[& \frac{dI_{Sa}^*}{dt} - \alpha_{2,a} e_{Ia} - \alpha_{1,a} \int_0^t e_{Ia}\, dt \\ & - \alpha_{0,a} \int_0^t \int_0^t e_{Ia}(\tau)\, d\tau dt \\ & + \gamma I_{Sa} - \eta\beta \psi_{Ra} - \beta n_p \omega \psi_{Rb} \Bigg] \end{aligned} \tag{23}$$

$$\begin{aligned} u_{sb} = \sigma L_S \Bigg[& \frac{dI_{Sb}^*}{dt} - \alpha_{2,b} e_{Ib} - \alpha_{1,b} \int_0^t e_{Ib}\, dt \\ & - \alpha_{0,b} \int_0^t \int_0^t e_{Ib}(\tau)\, d\tau dt \\ & + \gamma I_{Sb} - \eta\beta \psi_{Rb} + \beta n_p \omega \psi_{Ra} \Bigg] \end{aligned} \tag{24}$$

with $e_{Ia} = I_{Sa} - I_{Sa}^*$ and $e_{Ib} = I_{Sb} - I_{Sb}^*$. In the same way, we proposed to determine the control parameters by,

$$\alpha_{0,a} = p_a^3, \quad \alpha_{1,a} = 3p_a^2, \quad \alpha_{2,a} = 3p_a \tag{25}$$

$$\alpha_{0,b} = p_b^3, \quad \alpha_{1,b} = 3p_b^2, \quad \alpha_{2,b} = 3p_b \tag{26}$$

with $p_a, p_b > 0$. Also, we proposed to include an adaptive performance with the correct definition of these values by BSNN.

C. FLUX OBSERVER

A flux observer is implemented to improve the transient response of the control strategy,

$$\begin{aligned} \frac{d}{dt}\widehat{I}_{Sa} = & -\gamma \widehat{I}_{Sa} + \eta\beta \widehat{\psi}_{Ra} + \beta n_p \omega \widehat{\psi}_{Rb} \\ & + \frac{1}{\sigma L_S} u_{sa} + k_a e_a \end{aligned} \tag{27}$$

$$\begin{aligned} \frac{d}{dt}\widehat{I}_{Sb} = & -\gamma \widehat{I}_{Sb} + \eta\beta \widehat{\psi}_{Rb} - \beta n_p \omega \widehat{\psi}_{Ra} \\ & + \frac{1}{\sigma L_S} u_{sb} + k_b e_b \end{aligned} \tag{28}$$

$$\begin{aligned} \frac{d}{dt}\widehat{\psi}_{Ra} = & -\frac{R_R}{L_R}\widehat{\psi}_{Ra} - n_p \omega \widehat{\psi}_{Rb} + \frac{R_R M}{L_R}\widehat{I}_{Sa} \\ & + \left(\eta\beta + \frac{R_R M}{L_R}\right) e_a - \beta n_p \omega e_b \end{aligned} \tag{29}$$

$$\begin{aligned} \frac{d}{dt}\widehat{\psi}_{Rb} = & -\frac{R_R}{L_R}\widehat{\psi}_{Rb} + n_p \omega \widehat{\psi}_{Ra} + \frac{R_R M}{L_R}\widehat{I}_{Sb} \\ & + \left(\eta\beta + \frac{R_R M}{L_R}\right) e_b + \beta n_p \omega e_a \end{aligned} \tag{30}$$

where $e_a = I_{Sa} - \widehat{I}_{Sa}$ and $e_b = I_{Sb} - \widehat{I}_{Sb}$, and $\widehat{\ }$ denotes the estimated signal. Asymptotic estimation of the magnetic flux signals can be thus verified by employing the Lyapunov function

$$V = \frac{1}{2}e_a^2 + \frac{1}{2}e_b^2 + \frac{1}{2}e_{\psi a}^2 + \frac{1}{2}e_{\psi b}^2 \tag{31}$$

with

$$\begin{aligned} \frac{d}{dt}V = & -(\gamma + k_a)\, e_a^2 - (\gamma + k_b)\, e_b^2 \\ & - \frac{R_R}{L_R} e_{\psi a}^2 - \frac{R_R}{L_R} e_{\psi b}^2 \end{aligned} \tag{32}$$

The observer parameters must be then selected such as $k_a, k_b > -\gamma$. The magnetic flux estimation errors are represented as: $e_{\psi a} = \psi_{Ra} - \widehat{\psi}_{Ra}$ and $e_{\psi b} = \psi_{Rb} - \widehat{\psi}_{Rb}$. Also, these parameters can be tuned using neural networks to attain adaptive behavior, for instance, considering positive values. Also, it can be defined as constant by, $k_a = 5\gamma$, $k_b = 5\gamma$. The Lyapunov function described in this paper was introduced in our previously published work [16]. However, what sets this study apart is the reduced reliance on motor parameters. Here, the gains k_a and k_b are dynamically determined through a BSNN scheme, mirroring the methodology applied to determine gains in other controllers. The initial conditions of the flow observer could be selected depending on the characteristics of the induction motor data, for example, $\widehat{\psi}_{Ra}(0) = 1$, $\widehat{\psi}_{Rb}(0) = 0$. The other variables are specified at zero as initial conditions if the motor is considered turned off.

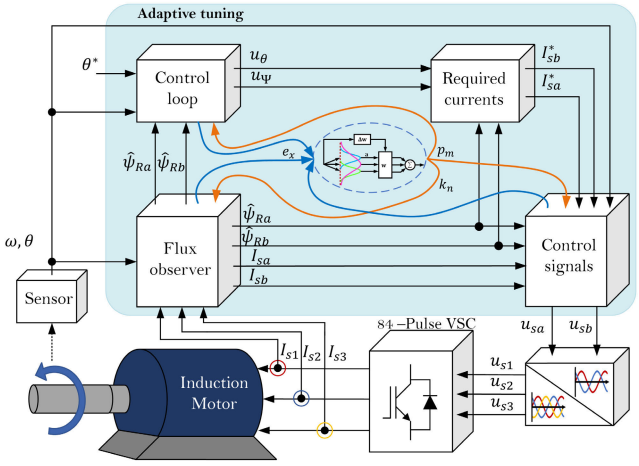

FIGURE 1. Proposed adaptive control scheme.

D. CONTROL SIGNALS

The required electrical currents trajectory, (22), including now the proposed flux observer leads to,

$$I_{Sa}^{*} = \frac{1}{\widehat{\Psi}}(\widehat{\psi}_{Ra}u_{\Psi} - \widehat{\psi}_{Rb}u_{\theta})$$
$$I_{Sb}^{*} = \frac{1}{\widehat{\Psi}}(\widehat{\psi}_{Rb}u_{\Psi} + \widehat{\psi}_{Ra}u_{\theta}) \tag{33}$$

where $\widehat{\Psi} = \widehat{\psi}_{Ra}^2 + \widehat{\psi}_{Rb}^2$.

Thus, the required control signals for the angular position are (14) and, considering the flux observer strategy, (15) is now defined by,

$$u_{\Psi} = \frac{L_R}{2R_R M}\left[\frac{d\Psi^*}{dt} - \alpha_{2,\Psi}e_{\Psi} - \alpha_{1,\Psi}\int_0^t e_{\Psi}dt - \alpha_{0,\Psi}\int_0^t\int_0^t e_{\Psi}(\tau)d\tau dt + \frac{2R_R}{L_R}\widehat{\Psi}\right] \tag{34}$$

also from (16) the flux error is determined using $e_{\Psi} = \widehat{\Psi} - \Psi^*$. Similar to other control parameters proposed in this paper, these $\alpha_{i,\Psi}$ are calculated dynamically by BSNN strategy. In summary, (23) and (24),

$$u_{sa} = \sigma L_S\left[-\alpha_{2,a}e_{Ia} - \alpha_{1,a}\int_0^t e_{Ia}dt - \alpha_{0,a}\int_0^t\int_0^t e_{Ia}(\tau)d\tau dt\right] \tag{35}$$

$$u_{sb} = \sigma L_S\left[-\alpha_{2,b}e_{Ib} - \alpha_{1,b}\int_0^t e_{Ib}dt - \alpha_{0,b}\int_0^t\int_0^t e_{Ib}(\tau)d\tau dt\right] \tag{36}$$

Fig. 1 presents the proposed adaptive control scheme where variable interaction can be appreciated. The observed errors, $e_x(t)$, serve as input to the BSNN, and depending on the operating condition of the IM, fine adjustments are made to the controller gains, p_m, and k_n, respectively.

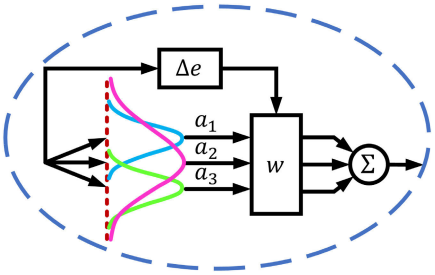

FIGURE 2. B-spline neural network with the proposed architecture.

E. ADAPTIVE PERFORMANCE OF CONTROL PARAMETERS

Nowadays, the high performance of digital microprocessors permits a combination of control strategies based on models with those based on measurements. However, dynamic performance must be guaranteed by the engineers in the design stage, also, with a compromise between low demand and computational complexity of those strategies to attain the desired behavior in a real-time environment.

In our proposed regulation scheme, the applicability of the proposed control scheme is extended to cover more demanding operation conditions different from those analyzed in the design stage, using an adaptive algorithm based on B-spline neural networks. Therefore, the control parameters $p_a, p_b, k_a, k_b, p_\theta$ and p_Ψ from (23), (24), (27), (28), (14), (34), respectively, could be determined adaptatively following actual dynamic operation condition of induction motor and specific load torque.

In this paper, a class of neural networks is selected due mainly to two powerful features: a) adaptability in a real-time environment considering the low computational demand in processing the output signal and, b) convergence capabilities of the learning rule. The first characteristic comes from its reduced architecture which consists of three stages, two layers consisting of inputs and outputs, respectively, and one hidden layer defined by basis functions' output, Fig. 2. The second feature is attained by the correct definition of knot vector which considers the expected values of input signals and so, establishes the shape of the basis functions together with the learning rate. Therefore, the proposed adaptive control gains, in this paper, are determined by,

$$p_m = y_p w, \text{ with } m = a, b, \theta, \Psi$$
$$k_n = y_k w, \text{ with } n = a, b \tag{37}$$

where y_p and y_k represent the outputs of the basis functions arranged in a row vector of an appropriate size for the number of neurons, as response of the input error, e_{Ia}, e_{Ib}, e_θ, e_Ψ, e_a and e_b, respectively. A key issue to attain the expected steady state and dynamic performance depends on the definition of basis functions. In this paper, the hidden layer of the artificial neural network architecture is defined by three neurons which include three uni-variate fourth-order functions known as basis functions. Due to the presented strategy the deviations of desired values are the inputs the three knot vectors are: i)

[-4.5 -1.5 1.5 4.5]; ii) [-0.05 0.35 0.75 0.115] and; iii) [-0.115 -0.75 -0.35 0.05]. The weighing factors are updated to attain the best dynamic performance adapting on their own to the new operating condition by the algebraic sum. In this case, using an architecture based on three neurons,

$$\begin{bmatrix} w_1 \\ w_2 \\ w_3 \end{bmatrix}^{km+1} = \begin{bmatrix} w_1 \\ w_2 \\ w_3 \end{bmatrix}^{km} + \begin{bmatrix} \Delta w_1 \\ \Delta w_2 \\ \Delta w_3 \end{bmatrix}^{km} \tag{38}$$

The weighing factor updating, $\Delta w^k m$, is determined by an instantaneous learning rule,

$$\Delta w^{km} = \frac{\zeta e_i^{km}(t)}{\|y^{km}(t)\|_2^2} y^{km}(t) \tag{39}$$

where km represents the current value; e_i represents the actual error (inputs); $\mathbf{y}(t)$ is the output of the basis functions; and ζ is the learning rate determined as a previous step. This update of the weighing factors is carried out with a low number of calculations due to the NN architecture, thus, is suitable for an online implementation. The learning rule convergence is guaranteed using a correct choice of the learning rate, ζ, typically defined with values smaller than one. In the offline stage (training stage) this value is adjusted very small like $1e-3$, after depending on the dynamic response of the inputs' changes can be adjusted with larger values. To attain the results presented in this paper the learning rate was defined as $\zeta = 2e-3$ considering the fast dynamics produced by the power electronic driver. The proposed control strategy begins with offline training of the BSNN with approximate values of control gains, and after, an online continuous learning process to adapt the control strategy performance to the unknown operation conditions of the induction motor.

In the design stage of the proposed position control algorithm, it is important to know approximated values of the motor parameters in advance, considering that the strategy begins from an approximated mathematical model. Besides that, information about typical operating conditions of the motor for a stable state and possible transient scenarios must be included in the offline training of the B-spline neural network scheme. The input signals should be normalized to develop a fine-tuning of the learning rate to ensure the convergence of the learning rule. In the offline training, if the BSNN is conditioned considering these main aspects of the position control algorithm, it will cope with unknown complex scenarios and nonmodeled dynamics not included in the control design stage as, for example, the dynamics of the power electronic components inside the VSC driver. Thus, it is possible to reduce the complexity and prior requirements of the controller structure while high dynamic performance facing unknown scenarios and uncertainties is guaranteed. The proposed control scheme exhibits high steady state and transient performance and desirable features for real-time applications such as robustness, adaptability, and low computational demand.

IV. DESIGN OF AN EFFICIENT ELECTRIC MOTOR DRIVE SYSTEM

A. TWO TO THREE PHASE CONVERTER

The coordinate reference for the three-phase power system is a three-axis system with a 120-degree phase shift. However, to facilitate the control implementation and analysis, the adoption of orthogonal coordinates is preferable.

In this paper, the transformation matrix used is,

$$\begin{bmatrix} u_{Sa} \\ u_{Sb} \\ u_{S0} \end{bmatrix} = \sqrt{\frac{2}{3}} \begin{bmatrix} 1 & -\frac{1}{2} & -\frac{1}{2} \\ 0 & \frac{\sqrt{3}}{2} & -\frac{\sqrt{3}}{2} \\ \frac{1}{\sqrt{2}} & \frac{1}{\sqrt{2}} & \frac{1}{\sqrt{2}} \end{bmatrix} \begin{bmatrix} u_{S1} \\ u_{S2} \\ u_{S3} \end{bmatrix}$$

if the three-phase source is balanced,

$$u_{S0} = \frac{1}{\sqrt{3}}(u_{S1} + u_{S2} + u_{S3})$$

The inverse transformation matrix is,

$$\begin{bmatrix} u_{S1} \\ u_{S2} \\ u_{S3} \end{bmatrix} = \sqrt{\frac{3}{2}} \begin{bmatrix} \frac{2}{3} & 0 & \frac{\sqrt{2}}{3} \\ -\frac{1}{3} & \frac{1}{\sqrt{3}} & \frac{\sqrt{2}}{3} \\ -\frac{1}{3} & -\frac{1}{\sqrt{3}} & \frac{\sqrt{2}}{3} \end{bmatrix} \begin{bmatrix} u_{Sa} \\ u_{Sb} \\ u_{S0} \end{bmatrix}$$

This transformation is applied in this work to achieve the presented results.

B. THE 84-MULTI-PULSE CONVERTER

An Electric Motor Drive System (EMDS) is a complex system that includes various components designed to control and regulate the operation of the induction motor. The purpose of the motor drive system is to efficiently convert electrical power into mechanical power, providing precise control over the motor's speed, torque, and position. A Voltage Source Converter (VSC) is typically used in EMDS to provide precise and efficient control on the speed and position of the shaft. By using the Neutral Point Reinjection (NPR) technique that involves injecting currents into the neutral point of the DC-link capacitors, several advantages arise. Examples of advantages are: enhancement of the voltage and current quality caused by the reduction of the harmonic distortion, increasing of the converter Efficiency, reduction in losses and stress on the switches, energy savings and increased overall system efficiency and dynamic performance. 84 pulses VSC has demonstrated to be a good implementation of the NPR technique [17], [18].

The signal involving the thee phase system is known as V_{module}, and it defined by (40), which means it is a constant for balanced systems with constant amplitude.

$$V_{module} = \sqrt{v_a^2 + v_b^2 + v_c^2} \tag{40}$$

It is of paramount importance to consider the significance of maintaining reduced amplitudes and lower frequencies for achieving effective speed and position control during startup and under varying the operating conditions. Voltage Source Converters (VSCs) play a crucial role in finely tuning amplitudes and frequencies to ensure efficient control. These

adjustments are particularly vital as deviations in torque or position demand substantial energy and can introduce significant voltage system distortions.

Synchronizing the phase and tracking of the required amplitude of a three-phase voltage signal to ensure the motor performance can be found in [16], [19], and [20]. Determining the frequency of this dynamic signal presents a challenging endeavor.

Phase-Locked Loop (PLL) uses the strategy presented in [16], [19], and [20] and it is illustrated in Eq. (41).

$$\omega t = 2\left[-tan^{-1}\left(\frac{\alpha}{\sqrt{\alpha^2+\beta^2}-\beta}\right)+\frac{\pi}{2}\right] \tag{41}$$

This equation presents α, and β which are obtained as the three-phase voltage signals in Stationary Reference Frame [21].

$$\begin{bmatrix}\alpha\\ \beta\end{bmatrix} = \frac{2}{3}\begin{bmatrix}1 & -\frac{1}{2} & -\frac{1}{2}\\ 0 & \frac{\sqrt{3}}{2} & -\frac{\sqrt{3}}{2}\end{bmatrix}\begin{bmatrix}a\\ b\\ c\end{bmatrix} \tag{42}$$

In (42) a, b, c are the three-phase balanced voltages or currents, as we can use this for obtaining the phase angle for both signals.

Using PLL, the Power Factor for phase-a is obtained as

$$\cos\left(\omega t_{v_a} - \omega t_{i_a}\right) \tag{43}$$

the argument $\left(\omega t_{v_a} - \omega t_{i_a}\right)$ is the difference between the angle of the voltage of phase-a $\left(\omega t_{v_a}\right)$ and angle of current of phase-a $\left(\omega t_{i_a}\right)$.

The complete controller comprises an 84-pulse VSC, with control signals determined in a digital processor using Equations (14), (34)-(39), and measured variables (Figure 1) including three-phase instantaneous currents and rotor position. The output signals of these equations involve basic mathematical operations suitable for straightforward implementation in common processors. The proposed 84-pulse VSC architecture exemplifies the efficient implementation of the developed position control strategy. While the presented results consider its dynamics, during the control design stage, these dynamics are treated as non-modeled or uncertain elements, successfully compensated by the adaptive strategy.

V. EVALUATION OF THE REGULATION PROPOSED STRATEGY

A. TEST CASE: 500 HP MOTOR

An asynchronous 500 hp motor is first used to demonstrate the scope of the proposed regulation scheme. The induction motor parameters are taken from [21] for 500 and 50 hp, respectively. In this case, some drastic operation conditions

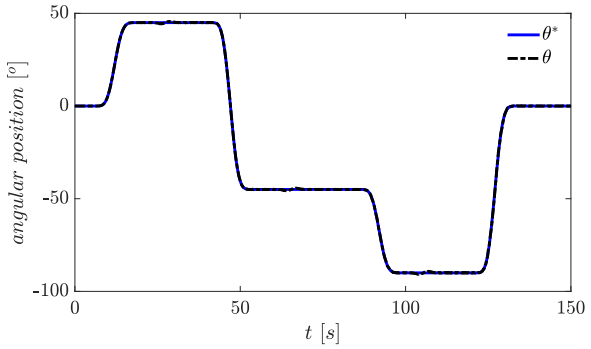

FIGURE 3. Trajectory tracking for angular position, case A.

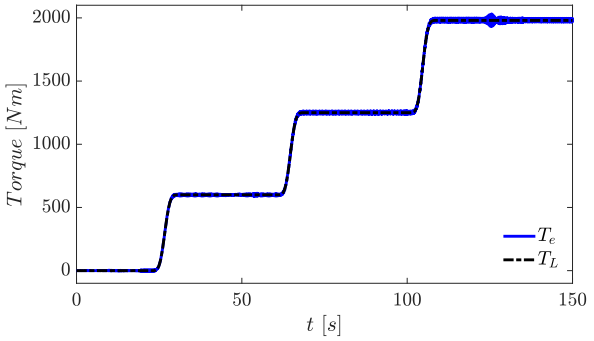

FIGURE 4. Demanded load torque and electric torque, case A.

are evaluated, and the required trajectory angle tracking is:

$$\theta^* = \begin{cases} 0^o & \text{if} \quad t < 5 \quad sec, \\ 45^o & \text{if} \quad 5 \le t < 40 \quad sec, \\ -45^o & \text{if } 40 \le t < 85 \quad sec, \\ -90^o & \text{if } 85 \le t < 120 \quad sec, \\ 0^o & \text{if} \quad t \ge 120 \quad sec \end{cases}$$

The trajectory from the initial to the final desired values is determined by a Bézier function, with a duration of 15 seconds for each transition, Fig. 3. It can be appreciated that the actual angular rotor position is tracking the required angular position although different requirements of load torque are presented.

Also, the motor is subject to variations in load torque with a transition of ten seconds from the initial to the final value, Fig. 4. At the beginning, the load torque is zero, after which, three new values of torque are demanding 600, 1250, and 1980 Nm, respectively. Notably, as the load torque approaches the nominal power, the adaptive control scheme effectively maintains the required angular rotor position. Despite these load torque variations, the scheme ensures other variables remain within physically permissible limits, exemplified by the electromagnetic torque aligning with the demanded load torque, as illustrated in Fig. 4.

On the other hand, Fig. 5 exhibits that the magnetic flux follows the optimal reference values for different load torque with a compromise between applied magnitude voltage and demanded electrical current. Thus, a reliable operation

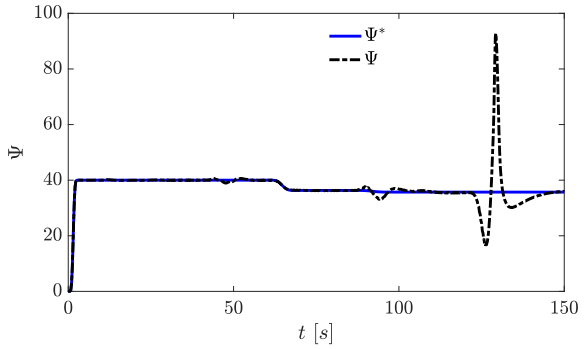

FIGURE 5. Required trajectory tracking for the magnetic flux, case A.

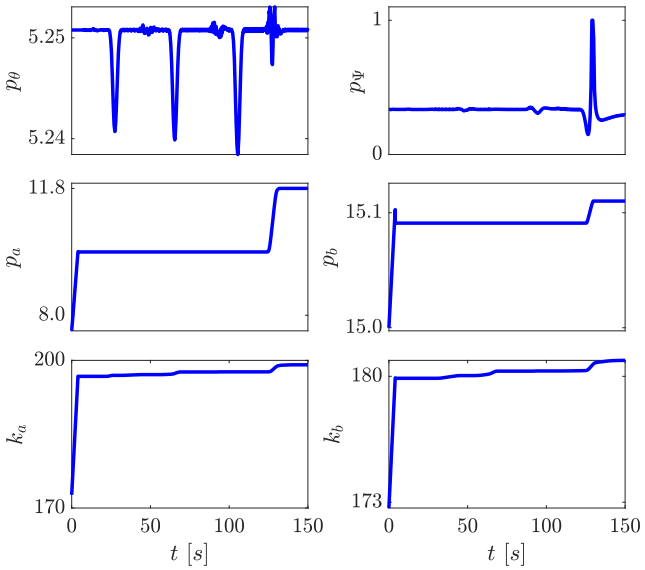

FIGURE 6. Dynamic evolution of the control gains, case A.

condition is guaranteed below the maximum allowable values for a steady state condition of this motor.

The control parameters are updated online by the proposed strategy based on B-spline neural networks. The behavior of the dynamic gains is shown in Fig. 6. Here, it presents the evolution of the control gain, p_θ, defined in (19), p_Ψ, in (20) due to the operation requirements of the induction motor. Also, the responses of the other four control gains associated with the dynamics of estimated electric currents, p_a, p_b, in (25) and (26), and k_a, k_b in flux observer scheme (27) and (28), respectively. All control gains are updated based on the requirements of the induction motor.

To attain the steady state and transient performance of the proposed controllers defined in section III, it is necessary to generate a three-phase input currents as a response to the load torque are presented in Fig. 7. The zoomed box illustrates the currents are very close to sinusoidal shape, which can be associated to a smooth behavior of the motor. The magnitude values are bounded within the nominal motor parameters.

The EMDS based in 84 pulses Voltage Source Converter described in IV-B is used to be able to feed the current

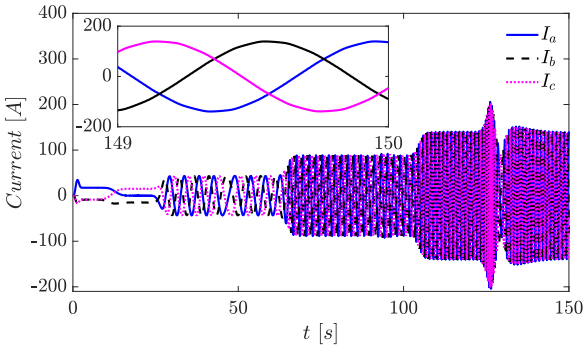

FIGURE 7. Electric currents demanded by the induction motor, case A.

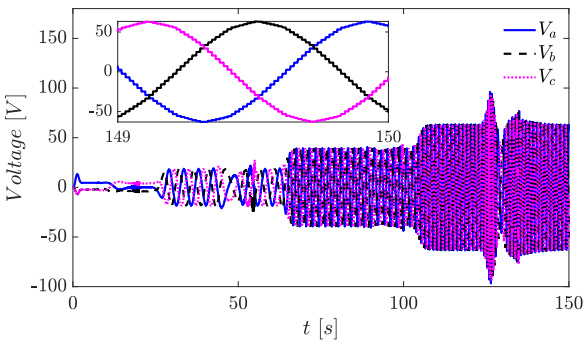

FIGURE 8. Applied three-phase input voltage, case A.

of Fig. 7. The variations of the are exhibited in Fig. 8. The adaptive control strategy or this proposal is evaluated including some fast dynamics associated with the power electronics components where the three-phase voltage is not exactly an alternating sinusoidal wave, but a staircase with low harmonic distortion, which is presented inside the zoomed box.

The EMDS has to be able to provide a voltage profile variable to produce the desired shaft position, as it is illustrated in Fig. 9. Controllers and voltage source converters, rely typically on filtered signals as the depicted in black on this figure for computing the desired output. The signal illustrated in blue is the one demanded by the system. It's important to clarify that the strategy of this paper presents the advantage of not incorporating filtering stages for the voltage module. The figure illustrate that, even with high-frequency variations on the voltage module, the resulting position is according to behavior the expected.

Torque variations are related to the frequency fluctuations during motor startup, and shifts in shaft position. To illustrate this, we incorporate Fig. 10. In this figure, the blue signal vividly displays abrupt transitions when the (PLL) detects the 2π phase angle. The black signal, in contrast, portrays the frequency variations after the application of a Low Pass Filter (LPF). It is important to emphasize that, in this study, we employ the unfiltered signal to illustrate our approach effectively, as it allows us to capture the intricate nuances of the system dynamics without any signal smoothing or

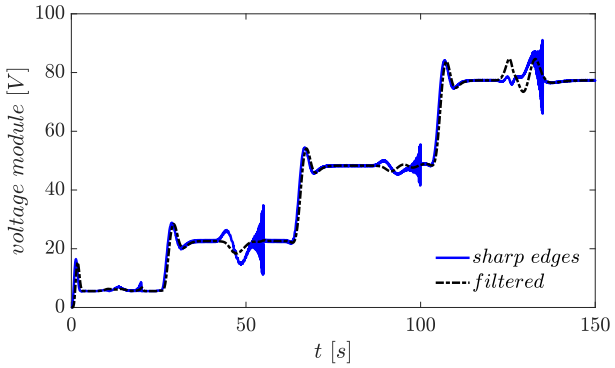

FIGURE 9. Voltage module for 500 hp induction motor.

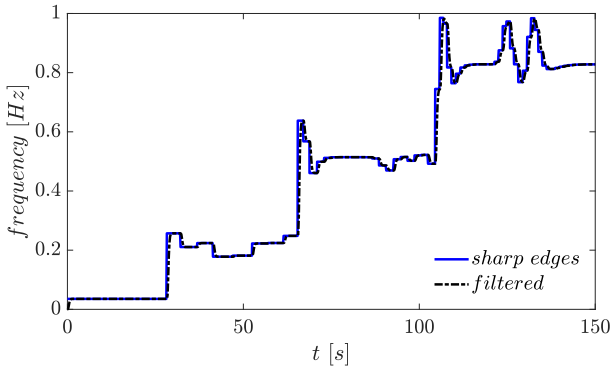

FIGURE 10. Frequency profile required for 500 hp induction motor.

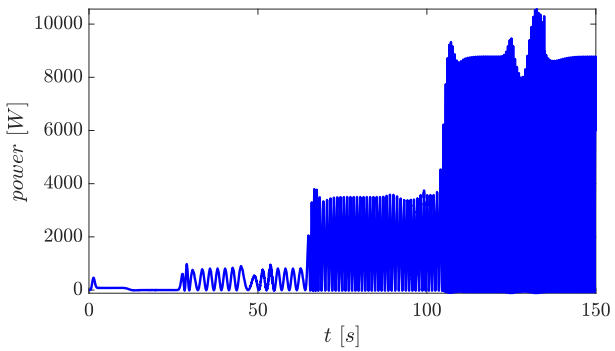

FIGURE 11. Power of Phase-*a* for 500hp induction motor.

filtering. Again, the figure intends to illustrate that the resulting position is according to expectations, even with high-frequency variations.

The devised approach takes into account a minimal reactive power for executing the designated tasks. In Fig. 11, the generated power is depicted, where segments below zero signify the reactive power. As depicted, nearly consistently, the power remains positive, indicating a negligible demand for reactive power.

Power factor is calculated with the strategy of (42), and presented in Fig. 12. As the reactive power is close to zero, the power factor is near to unity for most of the analyzed time.

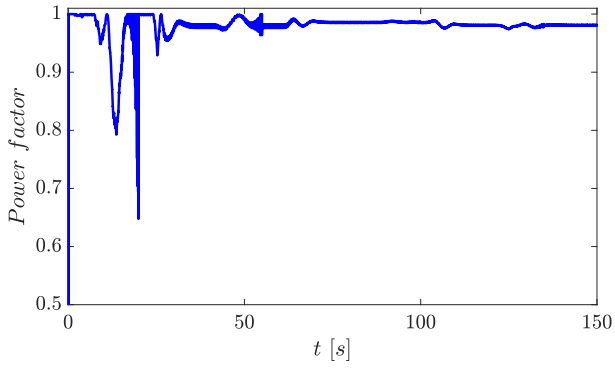

FIGURE 12. Power Factor for Phase-*a* for 500hp induction motor.

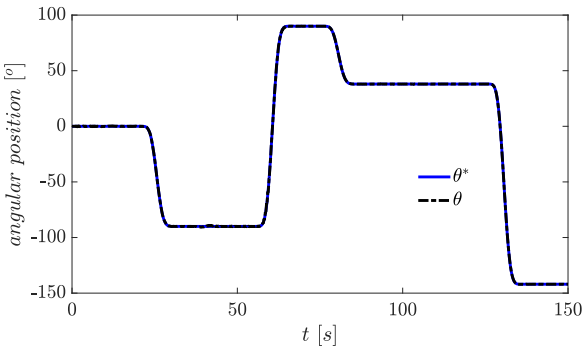

FIGURE 13. Trajectory tracking for angular position, case B.

B. TEST CASE: 50 HP MOTOR

In order to contrast the applicability of the regulation strategy and its adaptability to induction motors of different power and parameters, a 50 hp three-phase IM is used. In this case, different desired trajectories covering new desired angular rotor positions are defined, and drastic load demand requirements are used. Here the prerequisite of angular position is,

$$\theta^* = \begin{cases} 0^o & \text{if} \quad t < 20 \quad sec, \\ -90^o & \text{if } 20 \leq t < 55 \quad sec, \\ 90^o & \text{if } 55 \leq t < 75 \quad sec, \\ 38^o & \text{if } 75 \leq t < 125 \ sec, \\ 142^o & \text{if} \quad t \geq 125 \ sec \end{cases}$$

Following the case A, the angular position reference tracking is reached with high precision and avoiding high overshoots, as presented in Fig. 13.

Besides that, the system is subject to changes in load torque as depicted in Fig. 14. First, the load demands 49.5 Nm, then, a drastic increment of the load is presented to attain the full torque. After that, the load diminished one-third to attain a value of 132 Nm. Finally, an increase is exhibited to reach 171.6 Nm.

The electrical currents required to the expected behavior are within the limits for an induction motor of this power, Fig. 15, while the three-phase input voltage is presented in Fig. 16. The waveforms fulfill the requirements for induction

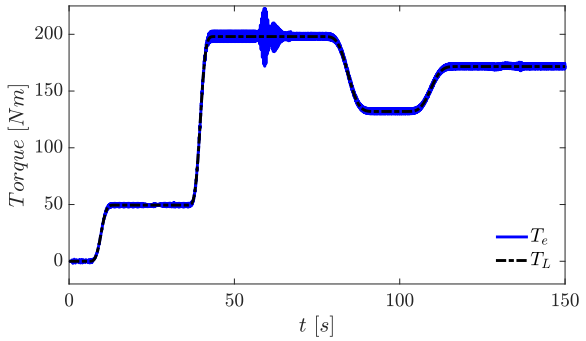

FIGURE 14. Demanded load torque and electric torque, case B.

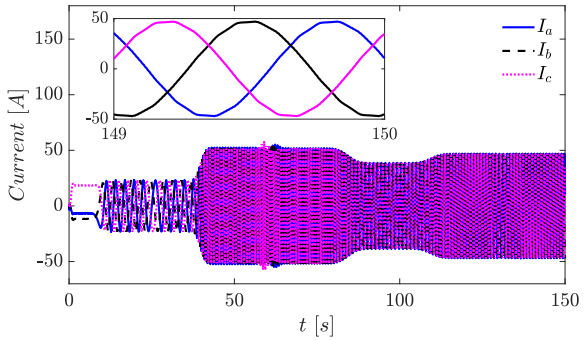

FIGURE 15. Electric currents demanded by the induction motor, case B.

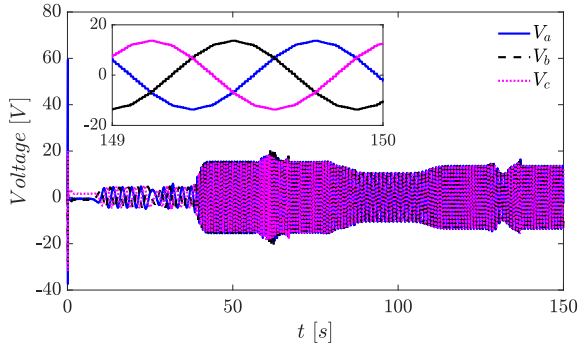

FIGURE 16. Applied three-phase input voltage, case B.

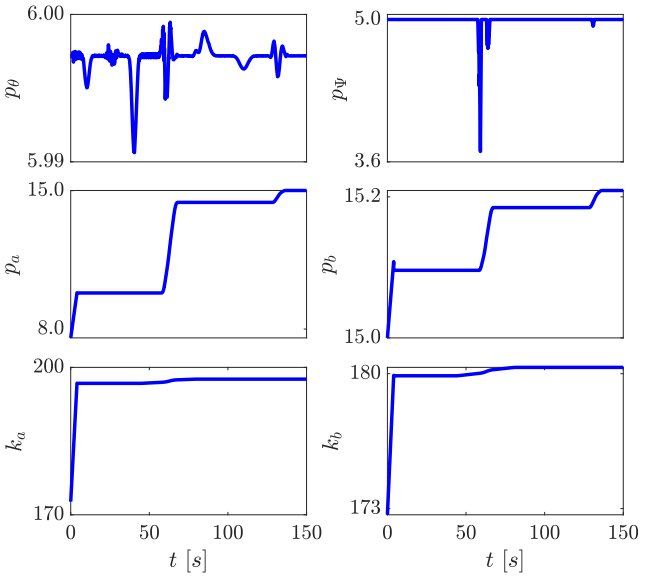

FIGURE 17. Dynamic evolution of the control gains, case B.

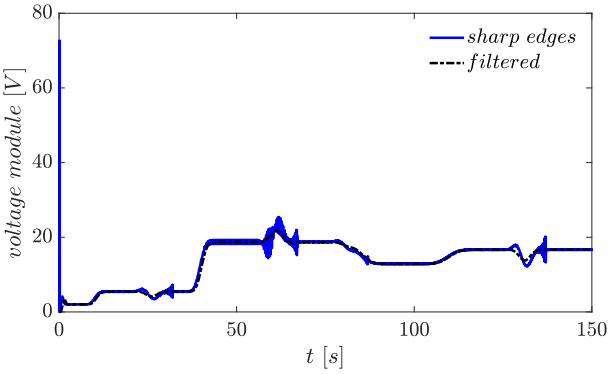

FIGURE 18. Voltage module for 50 hp induction motor.

motor controls considering applied voltages and demanding electrical currents. Also, with an adaptive control scheme as proposed in this paper, it is possible to reduce the dependence on previous knowledge of motor parameters.

The performance of the proposed control scheme for a 50 hp induction motor was attained with the same architecture of BSNN and parameters design the motor's parameters were replaced by the corresponding to this power. As can be seen, the behavior of this particular motor has high dynamic performance such as the 500 hp IM, thus, the adaptive control scheme fulfills the requirements for different power and parameters of induction motors for angular position control tasks. Thus, the dynamic evolution of the control gains is presented in Fig. 17. Two correspond to the internal control loop, also, two correspond to the control loop of electrical currents, and two of the flux observer. The values of the control gains begin with a predefined value determined by the previous stage offline (training rule), so their magnitudes are updated to guarantee the expected dynamic performance until a new steady state condition is reached. The results show more drastic changes when a transient event is presented, the learning rule updates the weighting factors attaining a fast transient response with stable performance. This strategy enhances the convergence to an optimum due to the search space is bounded by the basis functions and the learning rate analyzed in section III-E.

The variable voltage profile required to produce the desired shaft position, is portrayed in Fig. 18. Blue signal is the one used for the strategy presented on this paper, but black signal is added for comparison with traditional systems with low pass filters.

The frequency fluctuations for this case are illustrated in Fig. 19. As in previous case, the blue signal is the one used for the position tracking while the black uses a Low Pass Filter.

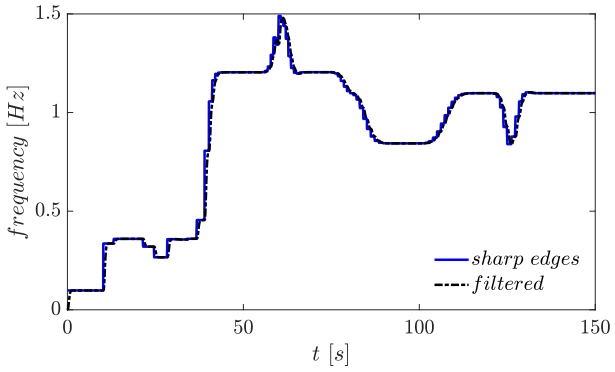

FIGURE 19. Frequency profile required for 50 hp induction motor.

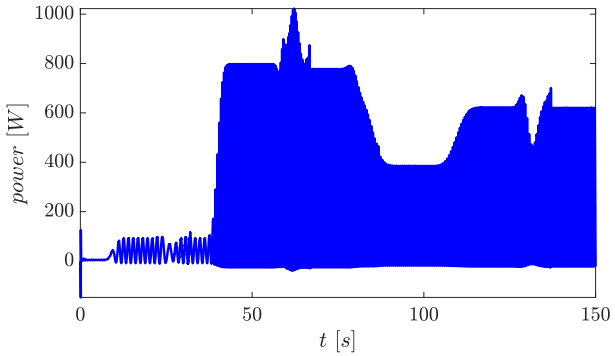

FIGURE 20. Power of Phase-a for 50hp induction motor.

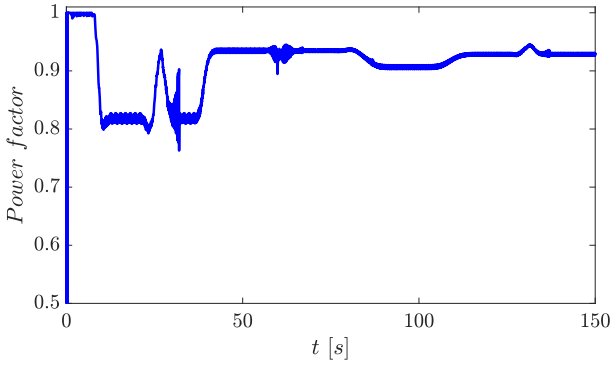

FIGURE 21. Power Factor for Phase-a for 50hp induction motor.

For this motor, a minimal reactive power for executing the designated tasks is required. In Fig. 20, the demanded power is depicted. The portions below zero indicate the reactive power required for operation.

Power factor presented in Fig. 21. As the reactive power demanded is higher than previous case, the power factor is lower, but most of the analyzed time is higher than 0.9.

VI. CONCLUSION

This paper proposes a control scheme for regulating rotor position in high-efficiency induction motors. The approach includes a thorough analysis of the performance of the voltage converter source, establishing a crucial link between control scheme and the power stage. Furthermore, the suggested control strategy facilitates seamless extension to motors of several power ratings. The uncertainties and non-modeled phenomena are dynamically compensated with the incorporation of B-spline neural networks working synergically with a strategy based on the model. Thus, the use of adaptive strategies makes it possible to cover a wide range of operation conditions and motor parameter variations. Several merit figures were included to verify the good the performance of the proposed strategy. Among them, the Power Factor attained was higher than 0.9 in both cases analyzed. Reactive Power was presented as the negative portion of the instantaneous power, and it was verified that is close to zero. The shape of the voltage and current was included to verify the closeness to the ideal sinusoidal signal, even-though stair cased signal was produced by the EMDS based in 84 pulses VSC.

Based on the analysis and results presented in this paper, the proposed position control scheme exhibits desirable features for highly demanding real-time applications, besides that, the requirements of detailed mathematical models were diminished. Accordingly, the immediate next step consists of the implementation of the whole system in the laboratory to verify the appropriateness of the proposal in particular study case. The mathematical operations related to the controller decision making will be translated to a digital controller.

ACKNOWLEDGMENT

The authors gratefully acknowledge the support of Universidad Panamericana Campus Guadalajara.

REFERENCES

[1] F. Bu, F. Xuan, Z. Yang, Y. Gao, Z. Pan, M. Degano, and C. Gerada, "Rotor position tracking control for low speed operation of direct-drive PMSM servo system," *IEEE/ASME Trans. Mechatronics*, vol. 26, no. 2, pp. 1129–1139, Apr. 2021.

[2] D. Mohanraj, J. Gopalakrishnan, B. Chokkalingam, and L. Mihet-Popa, "Critical aspects of electric motor drive controllers and mitigation of torque ripple—Review," *IEEE Access*, vol. 10, pp. 73635–73674, 2022.

[3] T. Li, J. Chen, Y. Wang, R. Ni, and Z. Liu, "Realization of smooth transition in hybrid PWM scheme for induction motor control," *IEEE Access*, vol. 7, pp. 162617–162628, 2019.

[4] M. M. Zirkohi, "Fast terminal sliding mode control design for position control of induction motors using adaptive quantum neural networks," *Appl. Soft Comput.*, vol. 115, Jan. 2022, Art. no. 108268.

[5] B. Dandil, "Fuzzy neural network IP controller for robust position control of induction motor drive," *Expert Syst. Appl.*, vol. 36, no. 3, pp. 4528–4534, Apr. 2009.

[6] Z. Tir, T. Orlowska-Kowalska, H. Ahmed, and A. Houari, "Adaptive high gain observer based MRAS for sensorless induction motor drives," *IEEE Trans. Ind. Electron.*, vol. 71, no. 1, pp. 271–281, Feb. 2023.

[7] Z. Yang, D. Wang, X. Sun, and J. Wu, "Speed sensorless control of a bearingless induction motor with combined neural network and fractional sliding mode," *Mechatronics*, vol. 82, Apr. 2022, Art. no. 102721. [Online]. Available: https://www.sciencedirect.com/science/article/pii/S095741582100180X

[8] T. Satheesh, R. Sakthivel, N. Aravinth, and H. R. Karimi, "Unified synchronization and fault-tolerant anti-disturbance control for synchronization of multiple memristor-based neural networks," *Int. J. Robust Nonlinear Control*, vol. 34, no. 4, pp. 2849–2864, Mar. 2024, doi: 10.1002/rnc.7112.

[9] R. Sakthivel, T. Satheesh, S. Harshavarthini, and D. J. Almakhles, "State estimation-based robust control design for periodic piecewise systems with time-varying delays," *Int. J. Syst. Sci.*, vol. 54, no. 2, pp. 405–422, Jan. 2023, doi: 10.1080/00207721.2022.2123264.

[10] O. Gulbudak, M. Gokdag, and H. Komurcugil, "Lyapunov-based model predictive control of dual-induction motors fed by a nine-switch inverter to improve the closed-loop stability," *Int. J. Electr. Power Energy Syst.*, vol. 146, Mar. 2023, Art. no. 108718. [Online]. Available: https://www.sciencedirect.com/science/article/pii/S0142061522007141

[11] P. C. Mavila and P. P. Rajeevan, "A reactive voltage compensation-based control scheme to extend speed range in five phase open-end winding induction motor drives," *IEEE Access*, vol. 11, pp. 126843–126856, 2023.

[12] S. Madanzadeh, S. S. H. Bukhari, and J.-S. Ro, "Multifunctional grid-connected voltage source inverter to drive induction motor operating with high-inertia load," *IEEE Access*, vol. 8, pp. 196765–196774, 2020.

[13] B. P. Reddy and N. S. Sundar, "Realization of a three-switch leg/phase inverter for nine-phase variable pole—Phase induction machine with phase grouping concepts," *IEEE Trans. Ind. Electron.*, vol. 71, no. 2, pp. 1181–1190, Feb. 2024.

[14] T. Jing and A. S. Maklakov, "A review of voltage source converters for energy applications," in *Proc. Int. Ural Conf. Green Energy (UralCon)*, Oct. 2018, pp. 275–281.

[15] S. Karmakar and B. Singh, "48-pulse voltage-source converter based on three-level neutral point clamp converters for solar photovoltaic plant," *IEEE J. Emerg. Sel. Topics Power Electron.*, vol. 10, no. 5, pp. 5894–5903, Oct. 2022.

[16] F. Beltran-Carbajal, R. Tapia-Olvera, A. Valderrabano-Gonzalez, and I. Lopez-Garcia, "Adaptive neuronal induction motor control with an 84-pulse voltage source converter," *Asian J. Control*, vol. 23, no. 4, pp. 1603–1616, Jul. 2021.

[17] A. Valderrabano-Gonzalez, F. Beltran-Carbajal, R. Tapia-Olvera, O. Aguilar-Mejia, and J. C. Rosas-Caro, "Design methodology for interfacing DERs to power systems through VSC," *Math. Problems Eng.*, vol. 2021, pp. 1–10, Oct. 2021.

[18] C. E. Castañeda, A. Valderrabano-Gonzalez, H. A. Gabbar, and O. A. Morfín, "Sliding mode with equivalent control for induction motor drive based on multi-pulse VSC," *Energies*, vol. 16, no. 13, p. 4866, Jun. 2023.

[19] F. Beltran-Carbajal, R. Tapia-Olvera, A. Valderrabano-Gonzalez, H. Yanez-Badillo, J. C. Rosas-Caro, and J. C. Mayo-Maldonado, "Closed-loop online harmonic vibration estimation in DC electric motor systems," *Appl. Math. Model.*, vol. 94, pp. 460–481, Jun. 2021.

[20] A. Valderrabano-Gonzalez, J. M. Ramirez, R. Tapia-Olvera, J. C. Rosas-Caro, J. M. Lozano-Garcia, and J. M. Gonzalez-Lopez, "Analysis and implementation of an 84-pulse STATCOM," in *Static Compensators (STATCOMs) in Power Systems*. Singapore: Springer, 2015, pp. 83–110.

[21] P. C. Krause, O. Wasynczuk, S. D. Sudhoff, and S. D. Pekarek, *Analysis of Electric Machinery and Drive Systems*. Hoboken, NJ, USA: Wiley, 2013, pp. 244–245.

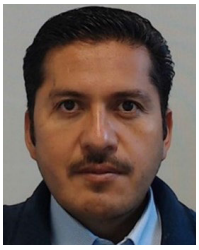

RUBEN TAPIA-OLVERA received the B.S. degree in electrical engineering from Instituto Tecnológico de Pachuca, Mexico, in 1999, and the M.Sc. and Ph.D. degrees in electrical engineering from CINVESTAV Guadalajara, Mexico, in 2002 and 2006, respectively. Currently, he is a full-time Professor with the Department of Electrical Energy, Universidad Nacional Autónoma de México (UNAM). His research interests include the modeling and control of electric machines and power systems with computational intelligence techniques.

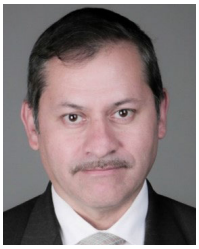

ANTONIO VALDERRABANO-GONZALEZ (Member, IEEE) received the B.S. degree in industrial electronics from Instituto Tecnológico de Puebla, Mexico, the M.Sc. degree in electronics from Instituto Nacional de Astrofísica, Óptica y Electrónica, Mexico, and the Ph.D. degree in electrical engineering from CINVESTAV Guadalajara, Mexico. He is currently a Professor with Universidad Panamericana Campus Guadalajara, Mexico. His research interests include power electronics, the control of power electronic converters, FACTS devices, and power quality.

FRANCISCO BELTRAN-CARBAJAL received the B.S. degree in electromechanical engineering from Instituto Tecnológico de Zacatepec, Mexico, and the Ph.D. degree in electrical engineering (mechatronics) from Centro de Investigación y Estudios Avanzados del Instituto Politécnico Nacional (CINVESTAV-IPN), Mexico City. He is currently a Titular Professor with the Energy Department, Universidad Autónoma Metropolitana (UAM), Unidad Azcapotzalco, Mexico City. His main research interests include vibration control, system identification, rotating machinery, mechatronics, and the automatic control of energy conversion systems.